

Emergence of: a reversed backward bifurcation , reversed hysteresis effect and backward bifurcation phenomenon in a COVID-19 mathematical model

Isaac Mwangi Wangari¹

¹Bomet University College

November 21, 2022

Abstract

A Coronavirus Disease 2019 (COVID-19) epidemiological model incorporating a boosted infection-acquired immunity and heterogeneity in infection-acquired immunity among recovered individuals is designed. The model is used to investigate whether incorporating these two processes can induce new epidemiological insights. Analytical findings reveal co-existence of multiple endemic equilibria on either regions divided by the fundamental threshold (control reproduction number). Numerical findings conducted to validate analytical results show that heterogeneity in infection-acquired immunity among recovered individuals can induce various bifurcation structures such as *reversed backward bifurcation*, *forward bifurcation*, *backward bifurcation* and *reversed hysteresis effect*. Moreover, numerical results show that *reversed backward bifurcation* is annihilated or switches to the usual *forward bifurcation* if infection-acquired immunity among recovered individuals with strong immunity is assumed to be everlasting. However, this is only possible if primary infection is more likely than reinfection. In case reinfection is more likely to occur than primary infection, *reversed backward bifurcation* structure switches to a *backward bifurcation* phenomenon. Further, longer duration of infection-acquired immunity does lead to COVID-19 decline over time but does not lead to flattening of the COVID-19 peak.

Emergence of: a *reversed backward bifurcation*, *reversed hysteresis effect* and *backward bifurcation phenomenon* in a COVID-19 mathematical model

Isaac Mwangi Wangari^{1,*}

1. Bomet University College, School of Pure and Applied Sciences, Department of Mathematics and Computing Science, P.O. Box 701-20400, Bomet, Kenya

Abstract

A Coronavirus Disease 2019 (COVID-19) epidemiological model incorporating a boosted infection-acquired immunity and heterogeneity in infection-acquired immunity among recovered individuals is designed. The model is used to investigate whether incorporating these two processes can induce new epidemiological insights. Analytical findings reveal co-existence of multiple endemic equilibria on either regions divided by the fundamental threshold (control reproduction number). Numerical findings conducted to validate analytical results show that heterogeneity in infection-acquired immunity among recovered individuals can induce various bifurcation structures such as *reversed backward bifurcation*, *forward bifurcation*, *backward bifurcation* and *reversed hysteresis effect*. Moreover, numerical results show that *reversed backward bifurcation* is annihilated or switches to the usual *forward bifurcation* if infection-acquired immunity among recovered individuals with strong immunity is assumed to be everlasting. However, this is only possible if primary infection is more likely than reinfection. In case reinfection is more likely to occur than primary infection, *reversed backward bifurcation* structure switches to a *backward bifurcation* phenomenon. Further, longer duration of infection-acquired immunity does lead to COVID-19 decline over time but does not lead to flattening of the COVID-19 peak.

Keywords: , Reexposure, immune boosting, Heterogeneity, reversed hysteresis effect, Reversed backward bifurcation

1. Introduction

The news about the spread of a novel coronavirus identified as severe acute respiratory syndrome coronavirus 2 (SARS-CoV-2) became ubiquitous across the globe in December 2019, and shortly thereafter the disease associated with the virus was named by World Health Organization (WHO) as Coronavirus Disease 2019 (or COVID-19) [1]. WHO declared COVID-19 a global pandemic on March 11, 2020 [2]. Official data from the WHO showed that, as of July 14, 2020, there were approximately 12,768,307 confirmed cases with 566,654 having succumbed to COVID-19 related complications [3]. Over a period of six months, about 105 million positive cases were confirmed, with 2.29 million deaths as of February 5, 2021. The pandemic continues to unfold, although at a slower pace in comparison to early onset of

*Corresponding author:

Email address: mwangiisaac@aims.ac.za (Isaac Mwangi Wangari)

COVID-19. Currently, there is a global concern regarding deciphering the extent of protection against emerging SARS-CoV-2 variants by pre-existing antibodies elicited as a result of natural infection or vaccination [4]. Consequently, numerous epidemiological modelling studies have attempted to incorporate infection mechanisms that account for COVID-19 post-infection possibilities. One being reinfection with either similar strain or a new variant of COVID-19, while the other possibility being COVID-19 recurrence (see [4] and the references therein).

The two most typical epidemiological models used to describe disease transmission dynamics include the SEIS (Susceptible-Exposed-Infection-Susceptible) and SEIR (Susceptible-Exposed-Infection-Recovered) [5, 6]. These two models are distinguishable from one another due to different assumptions made regarding immunity after infection [7]. For instance, for SEIR model recuperated individuals are assumed to have acquired infection derived immunity that is perfect and lasts throughout individuals life. These individuals are considered to be fully protected against infection with the same pathogen. On the other hand for SEIS models recovered individuals are assumed to acquire no immunity and immediately after recuperating remain susceptible to the pathogen they were previously infected with and at the same risk as before [7]. Infectious diseases with SEIS epidemiological characteristics include sexually transmitted diseases (STDs). For example, syphilis, gonorrhea, herpes simplex and chlamydia [8]. Contrary to both SEIS and SEIR infectious disease epidemiological characteristics, some diseases fall in between. That is convalescent immunity is not sufficient to protect an individual from future infection with a similar pathogen or closely related strain of the pathogen. This is evidenced by studies done on respiratory syncytial virus (RSV) which depict that infections render partial immunity and that the likelihood of being reinfected is decreased by about 70% for a period of six months following initial infection [9, 10, 11].

Similar to RSV, there are clinical studies that show that individuals who have recovered from COVID-19 can also be reinfected with previous COVID-19 variant or with the emerging COVID-19 variants (e.g., Delta, Omicron etc). For example [12] showed that overall protection after first episode of SARS-CoV-2 range between 77% and 83%. Other longitudinal study on immunological memory to SARS-CoV-2 showed that about 95% of recovered individuals retained immunity for a period of about eight months as evidenced by the measurements of antibodies, memory B cells and CD4 and CD8 T cells [13].

In the sequel there has been numerous epidemiological models that have attempted to study the impact of reinfection on overall COVID-19 dynamics. For instance the paper by [14] analysed COVID-19 transmission dynamics in Malaysia using an SIRS model. In their view the authors suggested that reinfection mechanism can be considered to be the process where recovered individuals lose the acquired infection derived immunity and revert to susceptible population. While this may have its epidemiological implications, perhaps they could have considered a scenario where recovered individuals interact with COVID-19 infectious individuals who are either infected with the same strain as they previously recovered from or a different COVID-19 variant. The omission of such vital infection mechanism probably hindered some enriching COVID-19 transmission dynamics. Further, the justification given by [14] that incubation period is not of significant importance in COVID-19 transmission dynamics and hence can be omitted is not strong enough given COVID-19 has a well known and documented intrinsic incubation period (see [1, 3, 15, 16] and the references therein). Batistela et al. [17] studied COVID-19 transmission dynamics using an SIRS model

but similarly assumed reinfection to be accounted by the loss of immunity among recovered individuals and finally returning to a susceptible state. Their mathematical analysis did not mention any possible dynamical behavior likely to be induced by reinfection mechanism, such as the phenomenon of *backward bifurcation*. Saha et al. [18] investigated dynamics of novel COVID-19 in the presence of co-morbidity with a possibility of reinfection of recovered individuals and found that reinfection could trigger a bistability phenomena. However, their paper did not consider a scenario where reinfection may boost an individual natural acquired immunity.

The paper by Rahman et al. [4] studied COVID-19 reinfection among naturally infected people and vaccinated individuals and found that although both cohorts were vulnerable to reinfection, individuals who naturally recovered from COVID-19 were less likely to be reinfected than individuals who were vaccinated. This clinical evidence raises an important question whether natural infection acquired-immunity (after recovery from COVID-19) is much stronger than vaccine induced immunity. Their paper pointed out that reinfected individuals (both naturally infected or vaccinated individuals) were less likely to suffer from severe disease. Their findings also suggested that a remarkable proportion of naturally infected or vaccinated individuals could be reinfected by the emerging COVID-19 variants. Their study did not hint a possibility of reinfection boosting an individual naturally acquired immunity despite the evidence that reinfected individuals were less likely to be hospitalized or experience high mortality as to individuals who suffer from COVID-19 for the first time.

The concept of immune boosting was initially hinted by Wearing and Rohani [19] in an attempt to estimate the duration of pertussis immunity using epidemiological signatures. However, their study did not reveal any epidemiological implications likely to be induced by incorporating boosted immunity infection mechanism in an epidemiological model. Recently, the research done by Le et al. [7] pointed out that re-exposed individuals may experience a boost to their waning immunity hence completely protecting them from reinfection. Again the study did not study in detail how boosted immunity may impact disease transmission dynamics. In the best of our knowledge no study on COVID-19 transmission dynamics has attempted to understand how boosted naturally acquired-immunity may impact future COVID-19 dynamics, particularly now COVID-19 prevalence is declining worldwide. Intriguingly, this decline in COVID-19 prevalence is being witnessed even among those countries that did not have an elaborate and successful vaccination mitigation strategy.

Reinfection is often if not always considered to be detrimental to the general population, especially if it leads to an increase in disease prevalence. Nevertheless, the overall dynamics of COVID-19 in presence of boosted immunity after reinfection with COVID-19 remains an important knowledge gap that has not been investigated so far using epidemiological modelling approach. In this paper we shall qualitatively and quantitatively explore a possibility where reinfection with COVID-19 is assumed to be multifaced. That is reinfection can either lead to an individual acquiring second episode of COVID-19 or can boost an individual infection-derived immunity such that an individual can transition from being partially immune to the status of temporary complete protection against COVID-19. Pertinent questions that will form the basis of our investigation include:

- (i) What is the epidemiological implication of boosted infection-acquired immunity? In

light of the revelation that reinfection among recovered individuals who have recuperated from COVID-19 can induce the phenomenon of backward bifurcation [18], we shall investigate whether incorporation of a boosted infection-acquired immunity mechanism can induce new bifurcation structures?

- (ii) Is there any epidemiological insights if there is heterogeneity in infection-acquired immunity among individuals who have recovered from COVID-19?
- (iii) Does duration of the infection-acquired immunity matter as far as COVID-19 transmission dynamics is concerned?

2. Model formulation

To investigate the stated questions we design a Kermack-McKendrick-type epidemiological model [20, 21], $SEIR_i$, ($i \in \{1, 2\}$) where the total human population at time, t denoted by $N(t)$ is partitioned into five mutually exclusive classes. That is susceptible individuals $S(t)$, individuals who are exposed to COVID-19 but are not yet infectious $E(t)$, infectious $I(t)$ which consist both symptomatic COVID-19 and asymptomatic COVID-19 infected individuals, recovered individuals who acquired partial infection-derived immunity $R_1(t)$ and recovered individuals $R_2(t)$ with full protection against COVID-19. This leads to

$$N(t) = S(t) + E(t) + I(t) + R_1(t) + R_2(t).$$

For the sake of mathematical tractability and simplification the following assumptions are made:

- Exposed individuals are asymptotically infected and cannot transmit COVID-19,
- Infectious individuals consist both symptomatic COVID-19 and asymptomatic COVID-19 infected individuals,
- Previous Covid-19 infection induces an infection-acquired immunity that can either be partial or strong enough to protect an individual from reinfection.
- Recovered individuals with strong infection-acquired immunity can gradually lose the acquired immunity and revert to a class of recovered individuals with partial immunity who are prone to reinfection.

Humans are recruited into the susceptible population at a constant rate Λ . Once susceptible individuals come into contact with infectious individuals in class $I(t)$, they acquire COVID-19 infection and proceed to exposed class at a rate λ , which is defined as:

$$\lambda = \frac{(1 - \omega\kappa)\beta I}{N}, \quad (1)$$

where parameter β represent effective contact rate. $0 < \kappa \leq 1$ represents proportion of the entire population that properly and consistently wear face masks while $0 < \omega \leq 1$ represents face masks effectiveness in preventing an individual from acquiring COVID-19 from

an infectious individual. The mathematical representation that track transmission dynamics of COVID-19 is defined by a system of nonlinear ordinary differential equations (2):

$$\begin{aligned}
\frac{dS}{dt} &= \Lambda - (\mu + \lambda)S, \\
\frac{dE}{dt} &= \lambda S + (1 - \phi)\delta\lambda R_1 - (\mu + \theta)E, \\
\frac{dI}{dt} &= \theta E - (\mu + d + \psi)I, \\
\frac{dR_1}{dt} &= (1 - f)\psi I + \alpha R_2 - (\mu + \delta\lambda)R_1, \\
\frac{dR_2}{dt} &= f\psi I + \phi\delta\lambda R_1 - (\mu + \alpha)R_2.
\end{aligned} \tag{2}$$

Individuals exposed to COVID-19 transition to the infectious class at a rate θE , ($\frac{1}{\theta}$, is the period exposed individuals sojourn in exposed class before becoming infectious, i.e., incubation period). Infectious individuals recover at a rate ψI . Recovery from COVID-19 is assumed to unfold into ways in that a proportion $f\psi I$ recover with a strong immunity and progress to R_2 class while the complimentary $(1 - f)\psi I$ recover with partial immunity and progress to R_1 class. Upon re-exposure to COVID-19 recovered individuals with partial immunity are prone to reinfection at a rate $\delta\lambda R_1$. $0 < \delta < 1$ is a modification parameter that account for reduction of infection among recovered individuals with partial immunity in relation to susceptible individuals. $\delta = 1$ imply recovered individuals are infected at the same rate as susceptible individuals while $\delta = 0$ indicate that recovered individuals with partial immunity are able to stage strong resistance against reinfection. It is assumed that recovered individuals with partial immunity respond differently to reinfection. That is a small proportion ϕ of individuals with partial infection-acquired immunity, their immunity is boosted upon reinfection and progress to R_2 class at a rate $\phi\delta\lambda R_1$ while the remainder follow the natural course of COVID-19 and progress to the exposed class at a rate $(1 - \phi)\delta\lambda R_1$. Strong infection-acquired immunity among recovered individuals (with strong immunity) is assumed to wane with time and these individuals join recovered individuals with partial immunity at a rate αR_2 . Humans in all classes are assumed to experience natural mortality at a rate μ . Individuals in infectious class, I experienced COVID-19 induced death at a rate dI . A summary of variables and parameters description is depicted in Table 1. A schematic diagram representing progression from one health status to another is shown in Figure (1).

3. Analysis of the model

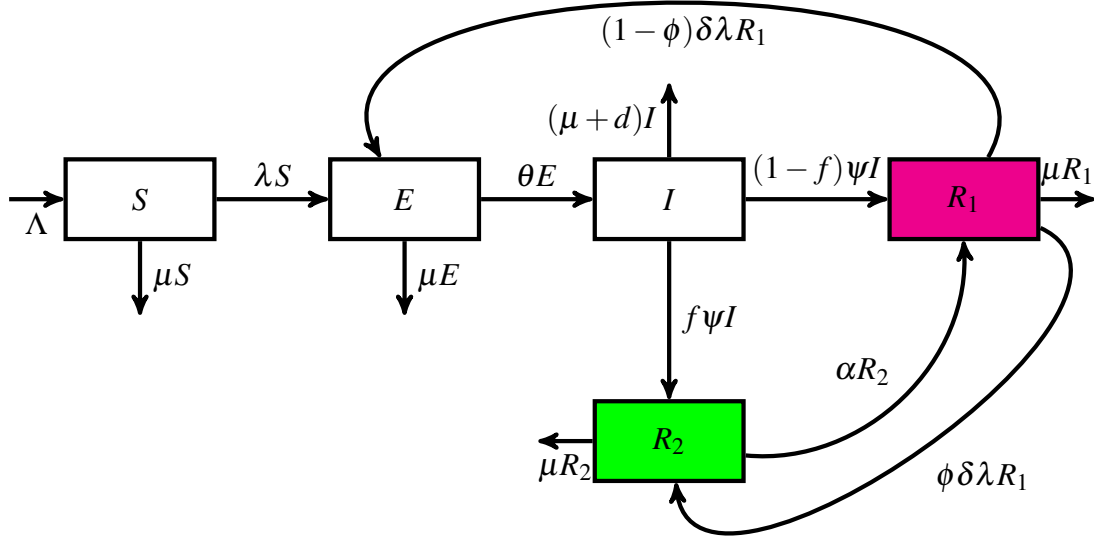


Figure 1: A flow diagram representing epidemiological status and the respective parameters which indicates rates of transition from one health status to another. The magenta filled compartment represent recovered individuals whose infection-acquired immunity is partial and these individuals can be reinfected upon re-exposure with COVID-19. The green filled compartment represents recovered individuals whose infection-acquired immunity is strong enough to resist reinfection.

3.1. Basic properties of the model

Positivity and boundedness of model trajectories

Given we are considering a human population it is imperative to show that all the variable states are nonnegative for all time, t . From model equation (2) we can deduce the following:

$$\begin{aligned}
 \frac{dS}{dt} \Big|_{\{S=0, E>0, I>0, R_1>0, R_2>0\}} &= \Lambda > 0, \\
 \frac{dE}{dt} \Big|_{\{S>0, E=0, I>0, R_1>0, R_2>0\}} &= \lambda S + (1 - \phi)\delta\lambda R_1 > 0, \\
 \frac{dI}{dt} \Big|_{\{S>0, E>0, I=0, R_1>0, R_2>0\}} &= \theta E > 0, \\
 \frac{dR_1}{dt} \Big|_{\{S>0, E>0, I>0, R_1=0, R_2>0\}} &= (1 - f)\psi I + \alpha R_2 > 0, \\
 \frac{dR_2}{dt} \Big|_{\{S>0, E>0, I>0, R_1>0, R_2=0\}} &= f\psi I + \phi\delta\lambda R_1 > 0.
 \end{aligned} \tag{3}$$

It is clear that all the rates in equation (3) are nonnegative on the boundary plane of the non-negative cone of \mathbb{R}^5 . The trajectories directions are inward on the boundary planes, thus if an

Table 1: Defination of variables and parameters for the COVID-19 model.

Variable	Description
S	Population of susceptible individuals
E	Population of exposed individuals who are not yet infectious
I	Population of both asymptomatic COVID-19 and symptomatic COVID-19 individuals
R_1	Population of recovered individuals with partial infection-acquired immunity who are vulnerable to reinfection
R_2	Population of recovered individuals with strong infection acquired immunity able to resist reinfection
Parameter	Description
Λ	Recruitment rate of humans
β	Effective contact rate
κ	Proportion of the entire susceptible population that properly and consistently wear face masks
ω	Efficacy of face masks in preventing acquisition of COVID-19 by susceptible individuals as well as to reduce the transmission of COVID-19 by infected individuals
θ	Transition rate from exposed class to infectious class
ψ	Recovery rate from COVID-19
f	Proportion of individuals who recover with strong infection acquired immunity
$(1 - f)$	Proportion of individuals who recover with partial infection acquired immunity
δ	Modification parameter that account for infection reduction among recovered individuals with partial immunity in relation to suceptible individuals
α	Rate at which recovered individuals lose the strong infection acquired immunity and revert to a class of recovered individuals with partial immunity
μ	Natural death rate
d	COVID-19 induced death rate
ϕ	Proportion of individuals who experience immune boosting upon re-exposure to COVID-19

initial condition within interior part of this cone is chosen, then all trajectories will remain within this cone for all future time. This proves the positivity of all the populations in the system (2).

To show boundedness of model solutions it can be noted that the total population is given as $N = S + E + I + R_1 + R_2$. Differentiating this equality yields

$$\frac{dN}{dt} = \Lambda - \mu N - dI. \quad (4)$$

From observation that $0 < S \leq N$, $0 < E \leq N$, $0 < I \leq N$, $0 < R_1 \leq N$, and $0 < R_2 \leq N$, it

follows that

$$\Lambda - (\mu + d)N \leq \frac{dN}{dt} < \Lambda - \mu N, \quad \text{hence, the following inequality:} \quad (5)$$

$$\frac{\Lambda}{\mu + d} \leq \liminf_{t \rightarrow \infty} N \leq \limsup_{t \rightarrow \infty} N \leq \frac{\Lambda}{\mu}.$$

This implies that $\limsup_{t \rightarrow \infty} N \leq \frac{\Lambda}{\mu}$ which shows that all model solutions are bounded above by $\frac{\Lambda}{\mu}$.

Theorem 1. *Let $\cap = \left\{ (S, E, I, R_1, R_2) \in \mathbb{R}_+^5 : 0 \leq S, E, I, R_1, R_2 \leq \frac{\Lambda}{\mu} \right\}$ be a set. Then \cap is a positively invariant and global attracting set of the model system (2).*

Proof: It follows from (5) that:

$$\frac{dN}{dt} \leq \Lambda - \mu N.$$

Since, $\frac{dN}{dt}$ is bounded above by $\Lambda - \mu N$, applying the standard comparison theorem in [22], it is easy to show that $N(t) \leq N(0)e^{-\mu t} + \frac{\Lambda}{\mu}(1 - e^{-\mu t})$. Specifically, the inequality holds if $N(0) \leq \frac{\Lambda}{\mu}$. This indicates that all trajectories of the model equation (2) with initial conditions originating from \cap remain in \cap for all time $t > 0$. Hence, \cap is a positively invariant and globally attracting set [23].

4. Local stability of disease-free equilibrium (DFE)

In the absence of COVID-19 infections, the model equation (2) has an intrinsic disease free equilibrium defined as

$$\mathcal{C}_0 = (\bar{S}, \bar{E}, \bar{I}, \bar{R}_1, \bar{R}_2) = \left(\frac{\Lambda}{\mu}, 0, 0, 0, 0 \right).$$

Applying the next generation operator method Diekmann et al. [24], Van den Driessche and Watmough [25] on the model equation (2) it is possible to investigate the linear stability of the DFE. From model equation (2), the matrices \mathcal{F} and \mathcal{V} which respectively represent new infections terms and transition terms are given by:

$$\mathcal{F} = \begin{pmatrix} 0 & (1 - \omega\kappa)\beta \\ 0 & 0 \end{pmatrix}, \quad \mathcal{V} = \begin{pmatrix} (\mu + \theta) & 0 \\ -\theta & (\mu + d + \psi) \end{pmatrix}.$$

The basic reproduction number which we shall define by R_c , is obtained from

$$R_c = \sigma(\mathcal{F}\mathcal{V}^{-1}) = \frac{(1 - \omega\kappa)\beta\theta}{(\mu + \theta)(\mu + d + \psi)}$$

where σ is the spectral radius of the next generation matrix $\mathcal{F}\mathcal{V}^{-1}$ (see [23, 25]). Following Van den Driessche and Watmough [25] we establish the following results

Lemma 1. *The DFE of the model equation (2) is locally asymptotically stable whenever $R_c < 1$ and unstable whenever $R_c > 1$.*

5. Existence of endemic equilibrium point (EEP)

If COVID-19 infections persists in any given community, then the disease becomes endemic leading to existence of an endemic equilibrium point. To determine the EEP we set all the expressions appearing at the right side of model equation (2) to zero and evaluate for steady states. Suppose

$$\mathcal{E}_1 = (S^*, E^*, I^*, R_1^*, R_2^*)$$

is any arbitrary endemic equilibrium point of model equation (2). Thus, equation (1) can be rewritten as

$$\lambda^* = \frac{(1 - \omega\kappa)\beta I^*}{N^*} \quad (6)$$

and N^* can be obtain from (4) as

$$N^* = \frac{\Lambda}{\mu} - \frac{dI^*}{\mu}.$$

Hence, from model (2) we can obtain

$$\begin{aligned} S^* &= \frac{\Lambda}{\mu + \lambda^*}, \\ E^* &= \frac{\lambda^* \Lambda}{(\mu + \lambda^*)(\mu + \theta)} + \frac{(1 - \phi)\delta\lambda^*}{(\mu + \theta)} R_1^*, \\ I^* &= \frac{\theta\lambda^* \Lambda (\mathcal{D}_1 + \lambda^* \mathcal{D}_2) + \theta^2 \lambda^{*2} \delta (1 - f) \psi (1 - \phi) (\mu + \alpha) \Lambda + \theta^2 \lambda^{*2} \delta \alpha f \psi (1 - \phi) (\mu + \lambda^*) \Lambda}{(\mu + \theta)(\mu + \lambda^*)(\mu + d + \psi)(\mathcal{D}_1 + \lambda^* \mathcal{D}_2)}, \end{aligned} \quad (7)$$

$$\begin{aligned} R_1^* &= \frac{(1 - f) \psi \theta \lambda^* \Lambda (\mu + \alpha) + \alpha f \psi \theta \lambda^* \Lambda (\mu + \lambda^*)}{(\mathcal{D}_1 + \lambda^* \mathcal{D}_2)(\mu + \lambda^*)}, \\ R_2^* &= \frac{f \psi \theta \lambda^* \Lambda}{(\mu + \alpha)(\mu + d + \psi)(\mu + \theta)} + \frac{f \psi \theta (1 - \phi) \delta \lambda^* + \phi \delta \lambda^* (\mu + \theta) (\mu + d + \psi)}{(\mu + \alpha)(\mu + d + \psi)(\mu + \theta)} R_1^*, \end{aligned}$$

where

$$\begin{aligned} \mathcal{D}_1 &= \mu(\mu + \alpha)(\mu + \theta)(\mu + d + \psi) > 0, \\ \mathcal{D}_2 &= \delta(\mu + d)(\mu + \theta)(\mu + \alpha(1 - \phi)) + \delta \psi \mu (\mu + \phi \theta) + \delta \mu \psi (1 - \phi) (\alpha + f \theta) > 0. \end{aligned}$$

Substituting (7) into (6) and after a tedious algebraic manipulation leads to the following polynomial expressed in terms of the force of infection λ^* :

$$\lambda^* [P_3(\lambda^*)^3 + P_2(\lambda^*)^2 + P_1\lambda^* + P_0] = 0, \quad (8)$$

where

$$\begin{aligned}
P_3 &= -d\theta^2\alpha f\psi(1-\phi)\delta, \\
P_2 &= \mu(\mu+d+\psi)\mathcal{D}_2 + \theta(\mu+\psi)\mathcal{D}_2 - d\theta^2\delta(1-\phi)(1-f)\psi(\mu+\alpha) - d\theta^2\mu\delta(1-\phi)\alpha f\psi \\
&\quad - \mu(1-\omega\kappa)\beta\theta^2\delta\alpha f\psi(1-\phi), \\
P_1 &= \mu(\mu+\theta)(\mu+d+\psi)\mathcal{D}_2 + \mu(\mu+d+\psi)\mathcal{D}_1 + \theta(\mu+\psi)\mathcal{D}_1 - (1-\omega\kappa)\mu\beta\theta\mathcal{D}_2 \\
&\quad - \mu(1-\omega\kappa)\beta\theta^2\delta(1-f)\psi(1-\phi)(\mu+\alpha) - \mu^2(1-\omega\kappa)\beta\theta^2\delta\alpha f\psi(1-\phi), \\
P_0 &= \mu(\mu+\theta)(\mu+d+\psi)\mathcal{D}_1[1-R_c].
\end{aligned}$$

Note that in polynomial (8), $\lambda^* = 0$ correspond to the DFE while the nonzero endemic equilibria are obtained from the cubic polynomial:

$$g(\lambda^*) = P_3(\lambda^*)^3 + P_2(\lambda^*)^2 + P_1\lambda^* + P_0 = 0. \quad (9)$$

It is clear that in polynomial (9), P_3 is always negative while P_0 can be either positive or negative depending on whether $R_c < 1$ ($R_c > 1$). The coefficients P_1 and P_2 can alternate between positive and negative values depending on the choice of parameter values. Hence, to determine all the possible number of endemic equilibria for model equation (2) we apply the Descartes' rule of signs on the cubic polynomial (9) for two cases. That is $R_c < 1$ and $R_c > 1$.

Case I: $R_c < 1$. Table 2 depict that whenever $R_c < 1$, model equation (2) can either have one positive endemic equilibrium point or three positive endemic equilibrium points. The existence of one or multiple endemic equilibrium points when $R_c < 1$ signals a possibility of bistability phenomenon. This is because for the bistability phenomenon to arise when $R_c < 1$, two endemic equilibria (where one is locally stable and the other unstable) need to coexist.

Table 2: Possible number of real positive roots for the case $R_c < 1$ determined by the signs of P_3, P_2, P_1 and P_0 .

P_3	P_2	P_1	P_0	Number of real positive roots
< 0	< 0	> 0	> 0	1 positive root
< 0	> 0	> 0	> 0	1 positive root
< 0	< 0	< 0	> 0	1 positive root
< 0	> 0	< 0	> 0	3 positive roots

Case II: $R_c > 1$. In this scenario P_0 is negative given $R_c > 1$ while P_3 as mentioned is always

Table 3: Possible number of positive roots for the case $R_c > 1$ which are determined by the signs of the coefficients P_3, P_2, P_1 and P_0 .

P_3	P_2	P_1	P_0	number of real positive roots
< 0	< 0	< 0	< 0	no positive root
< 0	< 0	> 0	< 0	2 positive roots
< 0	> 0	< 0	< 0	2 positive roots
< 0	> 0	> 0	< 0	2 positive roots

negative. Thus, the signs of the coefficients P_2 and P_1 determine the possible number of endemic equilibrium points for model equation (2). From Table 3 it can be seen that when R_c is greater than one, the model equation (2) have two endemic equilibria occurring concurrently. The coexistence of two endemic equilibrium points is one of the hallmark of the bistability phenomenon. Interestingly, the occurrence of bistability phenomenon for model equation (2) is exhibited when the control reproduction number is greater than one. The occurrence of the bistability phenomenon which in this case we shall refer to “reversed backward bifurcation” or “reversed bistability phenomeon” raises an important question that need further exploration. That is can we establish backward bifurcation threshold for a scenario where backward bifurcation occur when control reproduction number is greater than one?

5.1. Existence of bistability phenomenon

It is clear from Tables 2 and 3 that the model equation (2) exhibits bistability phenomenon when the control reproduction number is either less than one or greater than one. Hence, the following theorem follows:

Theorem 2. *Define*

$$\delta_c = \frac{\theta\psi[(1-f)\mu + \alpha] + \mu(\mu + \alpha)(\mu + d + \psi) + \mu\theta(\mu + \alpha)}{\theta\psi[(1-f)\mu + \alpha]}.$$

Then the Covid-19 model system (2)

- (i) Exhibits a reversed backward bifurcation phenomenon at $R_c = 1$ whenever $0 < (1 - \phi)\delta < \delta_c$
- (ii) Exhibits either a backward bifurcation phenomenon or a reversed hysteresis effect at $R_c = 1$ whenever $(1 - \phi)\delta > \delta_c$.

Proof: Using mathematical modelling insights, particularly center manifold theory Castillo-Chavez and Song [26] we establish a critical value that determine the type of bifurcation structures exhibited by model system (2) if crossed. For simplification purpose let $S = y_1, E = y_2, I = y_3, R_1 = y_4, R_2 = y_5$. Now model (2) in vector form can be written as $\frac{dY}{dt} = (f_1, f_2, f_3, f_4, f_5)$ where $Y = (y_1, y_2, y_3, y_4, y_5)^T$, so that

$$\begin{aligned} \frac{dy_1}{dt} &= f_1 = \Lambda - \frac{(1 - \omega\kappa)\beta y_1 y_3}{y_1 + y_2 + y_3 + y_4 + y_5} - \mu y_1, \\ \frac{dy_2}{dt} &= f_2 = \frac{(1 - \omega\kappa)\beta y_1 y_3}{y_1 + y_2 + y_3 + y_4 + y_5} + \frac{(1 - \phi)\delta(1 - \omega\kappa)\beta y_3 y_4}{y_1 + y_2 + y_3 + y_4 + y_5} - (\mu + \theta)y_2, \\ \frac{dy_3}{dt} &= f_3 = \theta y_2 - (\mu + d + \psi)y_3, \\ \frac{dy_4}{dt} &= f_4 = (1 - f)\psi y_3 + \alpha y_5 - \frac{\delta(1 - \omega\kappa)\beta y_3 y_4}{y_1 + y_2 + y_3 + y_4 + y_5} - \mu y_4, \\ \frac{dy_5}{dt} &= f_5 = f\psi y_3 + \frac{\phi\delta(1 - \omega\kappa)\beta y_3 y_4}{y_1 + y_2 + y_3 + y_4 + y_5} - (\mu + \alpha)y_5. \end{aligned} \tag{10}$$

Choosing β as the bifurcation parameter so that at $R_c = 1$, $\beta = \beta^* = \frac{(\mu + \theta)(\mu + d + \psi)}{(1 - \omega\kappa)\theta}$. Now the linearization matrix of model system (10) is computed by obtaining its Jacobian matrix

evaluated at the DFE \mathcal{E}_0 and considering that $\beta = \beta^*$. Hence,

$$J(\mathcal{E}_0)|_{\beta=\beta^*} = J_{\beta^*} = \begin{pmatrix} -\mu & 0 & -(1-\omega\kappa)\beta^* & 0 & 0 \\ 0 & -(\mu+\theta) & (1-\omega\kappa)\beta^* & 0 & 0 \\ 0 & \theta & -(\mu+d+\psi) & 0 & 0 \\ 0 & 0 & (1-f)\psi & -\mu & \alpha \\ 0 & 0 & f\psi & 0 & -(\mu+\alpha) \end{pmatrix}.$$

The eigenvalues of the Jacobian matrix $J(\mathcal{E}_0)|_{\beta=\beta^*}$ are easily computed using the Mathematica software and they include: $\lambda_1 = -(\mu+\alpha)$, $\lambda_2 = -\mu$, $\lambda_3 = -\mu$, $\lambda_4 = -2(d+\theta+2\mu+\psi)$ and $\lambda_5 = 0$. Observe that the Jacobian matrix $J(\mathcal{E}_0)|_{\beta=\beta^*}$ has a simple zero eigenvalue ($\lambda_5 = 0$) while all other eigenvalues have negative real part. Hence, the model system (10) has a hyperbolic equilibrium point which implies that we can proceed and apply the center manifold theory Castillo-Chavez and Song [26] to analyze dynamics of the transformed system near $\beta = \beta^*$. We now compute both right and left eigenvectors of the Jacobian matrix $J(\mathcal{E}_0)|_{\beta=\beta^*}$.

Eigenvectors of the $J(\mathcal{E}_0)|_{\beta=\beta^*}$.

The corresponding right and left eigenvectors of the jacobian matrix $J(\mathcal{E}_0)|_{\beta=\beta^*}$ associated with the zero eigenvalue are respectively given as:

$$\text{Right eigenvectors: } v_1 = -\frac{(1-\omega\kappa)\beta^*}{\mu}v_3, v_2 = \frac{(\mu+d+\psi)}{\theta}v_3, v_3 = v_3 > 0,$$

$$v_4 = \frac{\psi[(1-f)\mu+\alpha]}{\mu(\mu+\alpha)}v_3, v_5 = \frac{f\psi v_3}{(\mu+\alpha)},$$

Left eigenvectors: $w_1 = w_4 = w_5 = 0$, $w_2 = \frac{\theta}{(\mu+\theta)}w_3$, $w_3 = w_3 > 0$. Now the associated bifurcation parameters, a and b (see [26]) are described by:

$$a = \sum_{k,i,j=1}^5 w_k v_i v_j \frac{\partial^2 f_k(0,0)}{\partial y_i \partial y_j} \quad \text{and} \quad b = \sum_{k,i=1}^5 w_k v_i \frac{\partial^2 f_k(0,0)}{\partial y_i \partial \beta^*}.$$

For bifurcation parameter a the associated non-vanishing partial derivatives of the transformed model system (10) evaluated at DFE \mathcal{E}_0 are given by:

$$\frac{\partial^2 f_2(0,0)}{\partial y_2 \partial y_3} = \frac{\partial^2 f_2(0,0)}{\partial y_3 \partial y_2} = -\frac{2(1-\omega\kappa)\beta^*\mu}{\Lambda},$$

$$\frac{\partial^2 f_2(0,0)}{\partial y_3 \partial y_4} = \frac{\partial^2 f_2(0,0)}{\partial y_4 \partial y_3} = 2 \left(-\frac{(1-\omega\kappa)\beta^*\mu}{\Lambda} + \frac{(1-\phi)\delta(1-\omega\kappa)\beta\mu}{\Lambda} \right),$$

$$\frac{\partial^2 f_2(0,0)}{\partial y_3^2} = \frac{-2(1-\omega\kappa)\beta^*\mu}{\Lambda}.$$

Further, the non-vanishing partial derivatives associated to b are given by

$$\frac{\partial^2 f_1(0,0)}{\partial y_3 \partial \beta^*} = -\frac{(1-\omega\kappa)\mu^2}{\Lambda^2}, \quad \frac{\partial^2 f_2(0,0)}{\partial y_3 \partial \beta^*} = \frac{(1-\omega\kappa)\mu^2}{\Lambda^2}.$$

Thus bifurcation parameters a and b after a tedious algebraic manipulation are given as:

$$\begin{aligned}
a &= 2 \frac{\theta(1-\omega\kappa)\beta^*\mu\psi[(1-f)\mu+\alpha]}{\Lambda(\mu+\theta)\mu(\mu+\alpha)} \\
&\times \left((1-\phi)\delta - \frac{\theta\psi[(1-f)\mu+\alpha] + \mu(\mu+\alpha)(\mu+d+\psi) + \mu\theta(\mu+\alpha)}{\theta\psi[(1-f)\mu+\alpha]} \right), \\
&= 2 \frac{\theta(1-\omega\kappa)\beta^*\mu\psi[(1-f)\mu+\alpha]}{\Lambda(\mu+\theta)\mu(\mu+\alpha)} ((1-\phi)\delta - \delta_c), \quad \text{where} \tag{11}
\end{aligned}$$

$$\begin{aligned}
\delta_c &= \frac{\theta\psi[(1-f)\mu+\alpha] + \mu(\mu+\alpha)(\mu+d+\psi) + \mu\theta(\mu+\alpha)}{\theta\psi[(1-f)\mu+\alpha]} \\
b &= \frac{\theta}{(\mu+\theta)} \frac{(1-\omega\kappa)\mu^2}{\Lambda^2} w_3 v_3 > 0. \tag{12}
\end{aligned}$$

From Theorem 4.1 of Castillo-Chavez and Song [26] it follows that the COVID-19 model (2) will exhibit the phenomenon of a ‘‘reversed backward bifurcation’’ at $R_c = 1$ whenever parameter $a < 0$. That is if $0 < (1-\phi)\delta \leq \delta_c$.

Remark 1. *It is imperative to stress that for a normal backward bifurcation phenomenon to occur the bifurcation parameter a obtained using Center Manifold theory need to be nonnegative. However, for scenarios where (a) reinfection among recovered individuals with partial immunity is assumed to strengthen an individual immunity and (b) there is heterogeneity in immunological response to COVID-19 infection leading to disparity in the level of infection-acquired immunity then the requirement that bifurcation parameter a need to be nonnegative is not a requirement as depicted in Figure (2).*

Using the baseline parameters shown on Table 4 the condition for a ‘‘reversed backward bifurcation’’ to occur can be computed as $\delta(1-\phi) = 0.4999 \approx 0.5 < \delta_c = 1.0004 \approx 1$. It is apparent that the bifurcation parameter a according to Castillo-Chavez and Song [26] will be negative yet the emergence of a reversed backward bifurcation is observed as depicted in Figure 2(a). In Figure 2(a), $\beta^* = 0.212$ correspond to $R_c = 1$.

5.2. Nonexistence of a reversed backward bifurcation when $\phi = 1$ or $\delta = 0$

The biological interpretation for $\phi = 1$, in model equation (2), is that re-exposure to COVID-19 leads to a 100% boosted natural immunity among previously infected individuals who recovered with partial immunity. Consequently, these individuals progress to a class of recovered individuals who are protected against reinfection due to their strong immunity. Nonexistence of the bistability phenomenon can be shown by noting that if ϕ is set to one in the cubic equation (9), the equation reduces to a quadratic equation $g(\lambda^*)|_{\phi=1} = \bar{P}_2 \lambda^{*2} + \bar{P}_1 \lambda^* + P_0 = 0$ where

$$\begin{aligned}
D_2|_{\phi=1} &= \bar{D}_2 = \delta(\mu+d)(\mu+\theta)\mu + \delta\psi\mu(\mu+\theta) > 0, \\
\bar{P}_2 &= \mu(\mu+d+\psi)\bar{D}_2 + \theta(\mu+\psi)\bar{D}_2 > 0, \tag{13} \\
\bar{P}_1 &= \mu(\mu+d+\psi)D_1 + \theta(\mu+\psi)D_1 > 0, \\
P_0 &= \mu(\mu+\theta)(\mu+d+\psi)D_1(1-R_c).
\end{aligned}$$

Clearly, quadratic equation $g(\lambda^*)|_{\phi=1} = \bar{P}_2 \lambda^{*2} + \bar{P}_1 \lambda^* + P_0 = 0$ has only one change of signs (according to Descartes’ rule of signs) when $R_c > 1$ implying existence of one positive root.

On one hand there is no positive root when $R_c < 1$ since $P_0 > 0$, (hence no change of signs). Thus, we have the results:

Theorem 3. *The Covid-19 model equation (2) with $\phi = 1$ has:*

- (i) *Exactly one unique endemic equilibrium point when $P_0 < 0$, (i.e., $R_c > 1$),*
- (ii) *No endemic equilibrium point when $P_0 > 0$, (i.e., $R_c < 1$).*

Existence of one endemic equilibrium point when $R_c > 1$ indicates that the model system (2) will exhibit a forward bifurcation and not backward bifurcation phenomenon as illustrated in Figure 2(b) ($\phi = 1$ correspond to a solid blue curve) where parameter ϕ is set to one while all other parameters are the baseline parameters as shown in Table 4. The epidemiological implication of nonexistence of bistability phenomenon when $\phi = 1$ is that for a *reversed backward bifurcation* phenomenon to occur then boosted infection-acquired immunity as a result of re-exposure among recovered individuals with partial immunity need not be perfect. That is for a bistability phenomenon to arise, a fraction of recovered individuals (with partial immunity) after reinfection has to progress to the exposed class (i.e., follow natural course of COVID-19). This implies that if parameter ϕ lie within the interval $0 \leq \phi < 1$ then “reversed backward bifurcation” phenomenon arises (see Figure 2(a) where $\phi = 0.001 < 1$). This signals that if the natural-acquired immunity is boosted by re-exposure then complex COVID-19 transmission dynamics may be triggered.

Similarly, when $\delta = 0$ model system (2) cannot exhibit a “reversed backward bifurcation” since equation (9) reduces to a linear equation. That is

$$g(\lambda^*)|_{\delta=0} = P_{11}\lambda^* + P_0 = 0,$$

where $P_1|_{\delta=0} = P_{11} = \mu(\mu + d + \psi)\mathcal{D}_1 + \theta(\mu + \psi)\mathcal{D}_1 > 0$. This implies $\lambda^* = -P_0/P_1$. Thus, λ^* remains positive whenever $R_c > 1$. Consequently, in the absence of reinfection of recovered individuals with partial immunity a unique endemic equilibrium exists whenever $R_c > 1$ and no positive endemic equilibrium point exist whenever $R_c < 1$. Figure 2(b) (where $\delta = 0$ correspond to dashed black curve) depict that the model equation (2) will not exhibit a “reversed backward bifurcation” but rather a forward bifurcation. Interestingly, the bifurcation structures for $\delta = 0$ and $\phi = 1$ are topologically equivalent as depicted in Figure 2(b) where the two curves are superimposed.

Table 4: Represents model parameter values used in numerical simulations

Parameter	Baseline values	Range	Unit	Reference
Λ	5000	[500–5000]	day ⁻¹	[18]
β	0.35	[0.1–0.86]	day ⁻¹	[15, 18, 27]
κ	0.5	[0.1–0.65]	day ⁻¹	[18, 27]
ω	0.1	[0.1–0.5]	day ⁻¹	[18, 27]
θ	0.20	[0.11–0.25]	day ⁻¹	[27, 15]
ψ	0.20	$[\frac{1}{30}-\frac{1}{4}]$	day ⁻¹	[18, 28, 27, 29, 30]
f	0.10	[0.05–0.85]	day ⁻¹	[15]
δ	0.5	[0–1]	day ⁻¹	[15, 18]
α	$\frac{1}{2 \times 30}$	$[\frac{1}{3 \times 30}-\frac{1}{18 \times 30}]$	day ⁻¹	[12, 31, 28]
μ	$\frac{1}{65 \times 365}$	--	day ⁻¹	[18, 28]
d	0.001	--	day ⁻¹	Assumed
ϕ	0.001	[0–1]	day ⁻¹	Assumed

5.3. Global stability of the DFE in the presence of perfect boosted immunity i.e., $\phi = 1$

Theorem 4. *If boosted immunity is perfect ($\phi = 1$) the DFE \mathcal{E}_0 is globally asymptotically stable whenever $R_c < 1$.*

Proof: Consider the Lyapunouv candidate function;

$$\mathcal{L}(S, E, I, R_1, R_2) = \frac{\theta}{\mu + \theta} E + I. \quad (14)$$

The fact that $S, E, I, R_1, R_2 > 0$ implies that $\mathcal{L}(S, E, I, R_1, R_2) > 0$ and $\mathcal{L}(S, E, I, R_1, R_2) = 0$ at $E = I = 0$. Hence, we proceed to show that the time derivative of the Lyapunouv function (14) along the solutions of system (2) is less or equal to zero ($\dot{\mathcal{L}} \leq 0$).

$$\begin{aligned} \dot{\mathcal{L}} &= \frac{\theta}{\mu + \theta} \dot{E} + \dot{I}, \\ &= \frac{\theta}{\mu + \theta} \left[\frac{(1 - \omega\kappa)\beta IS}{N} - (\mu + \theta)E \right] + (\theta E - (\mu + d + \psi)I), \\ &= \frac{(1 - \omega\kappa)\beta \theta IS}{N(\mu + \theta)} - (\mu + d + \psi)I, \\ &= (\mu + d + \psi)I \left(\frac{(1 - \omega\kappa)\beta \theta S}{N(\mu + \theta)(\mu + d + \psi)} - 1 \right) \end{aligned}$$

Note that, due to infection $S(t)$ is diminished at any time $t \geq 0$. Let $S \leq \frac{\Lambda}{\mu}$ and $N \leq \frac{\Lambda}{\mu}$ then

$$\begin{aligned} \dot{\mathcal{L}} &\leq (\mu + d + \psi)I \left(\frac{(1 - \omega\kappa)\beta \theta}{(\mu + \theta)(\mu + d + \psi)} - 1 \right), \\ &= (\mu + d + \psi)I(R_c - 1). \end{aligned}$$

It can be observed that $\mathcal{L} = 0$ when $E = I = 0$ and $\mathcal{L} \leq 0$ whenever $R_c \leq 1$. Hence, by applying Lassalle’s invariance principle the obtained result show that \mathcal{E}_0 is globally asymptotically stable (g.a.s) in \cap . The epidemiological implication of DFE, \mathcal{E}_0 being g.a.s is that COVID-19 will be eliminated from the community if the control reproduction number R_c is maintained (or decreased) to a value below unity.

5.4. Impact of increasing proportion of individuals whose infection-derived immunity is boosted.

Varying proportion of individuals whose infection-derived immunity is boosted between values within the range $\phi \in [0, 1)$ has a significant impact on COVID-19 transmission dynamics. For example increasing parameter ϕ from $\phi = 0.001$ to $\phi = 0.001 \times 50$ shifts the reversed backward bifurcation to the right as well as widens endemic curves (see Figure 2(c)). Surprisingly, when ϕ is increased to a value exactly equal to 1 the *reversed backward bifurcation* switches to the usual *forward bifurcation* as depicted in Figure 2(b). Thus, disparity in immunological response towards reinfection among recovered individuals is vital in emergence of complex COVID-19 transmission dynamics. Epidemiologically this suggests that as long as a fraction of reinfected individuals transition to exposed class while the complementary progress to R_2 class (recovered individuals with strong but temporary immunity), then model system (2) will always exhibit a *reversed backward bifurcation*.

5.5. Reinfection does not boost infection-acquired immunity among recovered individuals with partial immunity ($\phi = 0$)

Under the assumption that reinfection with COVID-19 does not boost an individual infection-acquired immunity, this can be epidemiologically interpreted to imply $\phi = 0$. That is upon re-exposure with COVID-19 recovered individuals with partial immunity respond negatively (i.e., individuals experience a second episode of COVID-19-reinfection) and thus follow the natural course of COVID-19. In this scenario the cubic equation (9) remains a third degree polynomial and the number of possible endemic equilibria can again be determined by Tables 2 and 3. Figure 2(f) which is generated by using baseline parameter values in Table 4 except $\phi = 0$ show that the model system (2) exhibits a “reversed backward bifurcation” phenomenon.

5.6. Impact of varying duration of COVID-19 immunity on reversed backward bifurcation structure

Figure 2(e) show the impact of increasing duration of temporary infection-acquired immunity. For a short duration of infection-acquired immunity (about two months (60 days)) the reversed backward bifurcation occur for a narrow range of β values. Further, increasing duration of infection acquired immunity (from 2 months to six months and then to a year) the bifurcation structures are shifted to the right meaning reversed backward bifurcation occur for a wider range of effective contact rate values. Moreover, there is widening of the bifurcation curves implying an increase in the force of infection. This implies that COVID-19 infection-acquired immunity that is not permanent will actually complicate COVID-19 transmission dynamics.

5.7. *Permanent infection acquired immunity among recovered individuals in R_2 class (i.e., $\alpha = 0$)*

Here we consider a scenario where recovered individuals with strong immunity do not lose their infection-acquired immunity throughout their life time. Epidemiologically this implies $\alpha = 0$. Thus, setting $\alpha = 0$, the cubic equation (9) reduces to a quadratic equation:

$$h(\lambda^*) = C_2 \lambda^{*2} + C_1 \lambda^* + C_0 = 0, \quad (15)$$

where

$$\begin{aligned} C_2 = P_2|_{\alpha=0} &= \mu(\mu + d + \psi)\mathcal{D}_{22} + \theta(\mu + \psi)[\delta\psi\mu(\mu + \phi)\theta + \delta\mu\psi(1 - \phi)f\theta] \\ &\quad + \theta\delta\mu^2(\mu + \psi)(\mu + \theta) + \theta(\mu + \psi)\delta\mu^2d + \theta^2\mu^2\delta\mu d + d\theta^2\delta\psi\mu > 0, \\ C_1 = P_1|_{\alpha=0} &= \mu^3(\mu + d + \psi)^2(\mu + \theta) + \theta\mu^3(\mu + \theta)(\mu + d + \psi) \\ &\quad + \mu(\mu + \theta)(\mu + d + \psi)\mathcal{D}_{22}[1 - R_c] \\ &\quad + \theta\psi\mu^2(\mu + \theta)(\mu + d + \psi)[1 - \delta(1 - \phi)(1 - f)R_c], \\ C_0 = P_0|_{\alpha=0} &= \mu(\mu + \theta)(\mu + d + \psi)\mathcal{D}_{11}[1 - R_c], \text{ and} \end{aligned}$$

$$\begin{aligned} \mathcal{D}_{11} = \mathcal{D}_1|_{\alpha=0} &= \mu^2(\mu + \theta)(\mu + d + \psi) > 0, \\ \mathcal{D}_{22} = \mathcal{D}_2|_{\alpha=0} &= \delta\mu(\mu + d)(\mu + \theta) + \delta\psi\mu(\mu + \phi\theta) + \delta\mu\psi(1 - \phi)f\theta. \end{aligned}$$

Note that in the quadratic equation (15) the coefficient C_2 is always greater than zero. C_1 is also positive whenever $R_c < 1$ and δ is restricted within the interval $(0 \leq \delta < 1)$. This is because the term $\delta(1 - \phi)(1 - f)R_c$ is a product of terms that are less than one. C_0 is positive whenever $R_c < 1$ and negative when $R_c > 1$. Thus, under this scenario there is only one change of signs according to the Descartes rule of signs. Hence, the quadratic equation (15) will have one positive root. Plotting force of infection at equilibrium, λ^* against infective contact rate β will result to the well known forward bifurcation.

However, if δ takes values that are larger than one, the term $\delta(1 - \phi)(1 - f)R_c$ may become greater than one even though $R_c < 1$ hence leading to $C_1 < 0$. Consequently, the quadratic equation can have two change of signs for values of $\delta > 1$. In this case equation (15) will have two positive roots whenever $R_c < 1$. The coexistence of two positive endemic equilibrium points when the control reproduction number is less than one is the feature of the phenomenon of *backward bifurcation* where one endemic equilibrium point is stable and the other is unstable.

It is observed that if the COVID-19 infection-acquired immunity is everlasting (i.e., $\alpha = 0$, shown by a blue solid curve in Figures 2(e) and 3(a)) among recovered individuals with strong immunity then the *reversed backward bifurcation* collapses to either a *forward bifurcation* for values of δ restricted within the interval $0 < \delta < 1$ or a backward bifurcation phenomenon arises for $\delta > 1$ as indicated in the Figure 3(b). That is the *reversed backward bifurcation* structure is annihilated by permanent infection-acquired immunity among recovered individuals with strong immunity. Hence, the gradual loss of infection-acquired immunity among individuals with strong immunity is detrimental to the measures put in place to combat COVID-19 as this may trigger complex bifurcation structures. This also suggests that

developing vaccines that render permanent protection against COVID-19 reinfection is vital in mitigating COVID-19 proliferation. This is because reinfection will be difficult to occur and if it occurs it will be relatively low such that by reducing the control reproduction number below one, COVID-19 will not be able to spread (this is the case with the *forward bifurcation*). Moreover it is imperative to stress that if reinfection among recovered individuals with partial immunity occur faster than primary infection (i.e., $\delta > 1$), then even in the presence of permanent immunity among individuals in R_2 class, backward bifurcation phenomenon may arise (see Figure 3(b)). Although it is less likely, this possibility cannot be entirely ruled out given the current evidence of COVID-19 infection breakthrough among previously recovered individuals Rahman et al. [4]. In this scenario it will be very difficult to control COVID-19 due to the fact that COVID-19 will spread even when $R_c < 1$ as can be observed in Figure 3(b).

Given we have investigated the two extreme values of ϕ (i.e., $\phi = 0$ and $\phi = 1$) we can now argue that the presence of complex bifurcation structures exhibited by model system (2) are not entirely triggered by boosted infection-derived immunity among recovered individuals but also due to heterogeneity in recovery among COVID-19 infectious individuals. That is individual immunological response to COVID-19 after infection may lead to unexpected COVID-19 transmission dynamics. That is the key trigger of the emergence of a reversed backward bifurcation is due to the differences in the level of infection-acquired immunity among recovered individuals. However, for the heterogeneity among recovered individuals to induce complex bifurcation structures (i.e., *reversed backward bifurcation* and *reversed hysteresis effect*) reinfection has to occur among recovered individuals with partial immunity (i.e., $\delta \neq 0$) and recovered individuals with strong infection-acquired immunity have to gradually lose their immunity (i.e., $\alpha \neq 0$).

5.8. Impact of presence or absence of heterogeneity in infection-acquired immunity among recovered individuals

Parameter f which actually determine the proportion of recovered individuals which either go to R_1 or R_2 classes, if decreased leads to a pronounced “reversed backward bifurcation” (i.e., it is bifurcation structure is shifted to the right) as well as shrinking of the bifurcation curves (as shown in Figure 2(d)). Further, if f is increased the “reversed backward bifurcation” shifts to the left (or is being diminished) but the bifurcation curves widen (or endemic curve shifts upward). Thus, there is an epidemiological advantage if more individuals in the community recover with weak or partial protective immunity. This is because *reversed backward bifurcation* phenomenon will occur for β values that are actually close to β^* or will occur to values of R_c that are close to one. Furthermore, widening of the bifurcation curves imply an increase in the force of infection and subsequently an increase in COVID-19 prevalence. We note that for the intermediate values of parameter f (i.e., $0 < f < 1$) the phenomenon of *reversed backward bifurcation* will always occur.

We now consider whether the reversed backward bifurcation can be annihilated by omitting heterogeneity in recovery. That is by assuming that after recovery all individuals progress to either R_1 class or R_2 class. This can be epidemiologically interpreted to mean that $f = 0$ or $f = 1$, respectively. Figure 4(a) show that by setting $f = 0$ while all other parameters remain as shown in the Table 4, the phenomenon of reversed backward bifurcation switches

to the usual *forward bifurcation*. Hence, if infected individuals all recover with weak/partial infection-acquired immunity *reversed backward bifurcation* does not occur. However, it is clear from Figure 4(a) that the COVID-19 prevalence will remain high.

On one hand, if parameter f is set to one which imply that all recovered individuals recover with strong temporary infection-acquired immunity, a pronounced *reversed backward bifurcation* occur as indicated in Figure 4(b). That is COVID-19 pandemic will unfold in two different endemic curves whenever $R_c > 1$, where one is stable (shown by a solid blue curve in Figure 4(b)) and the other is unstable (shown by a solid red curve in Figure 4(b)). Thus there is a huge structural change in the bifurcation structure when the heterogeneity in recovery is omitted.

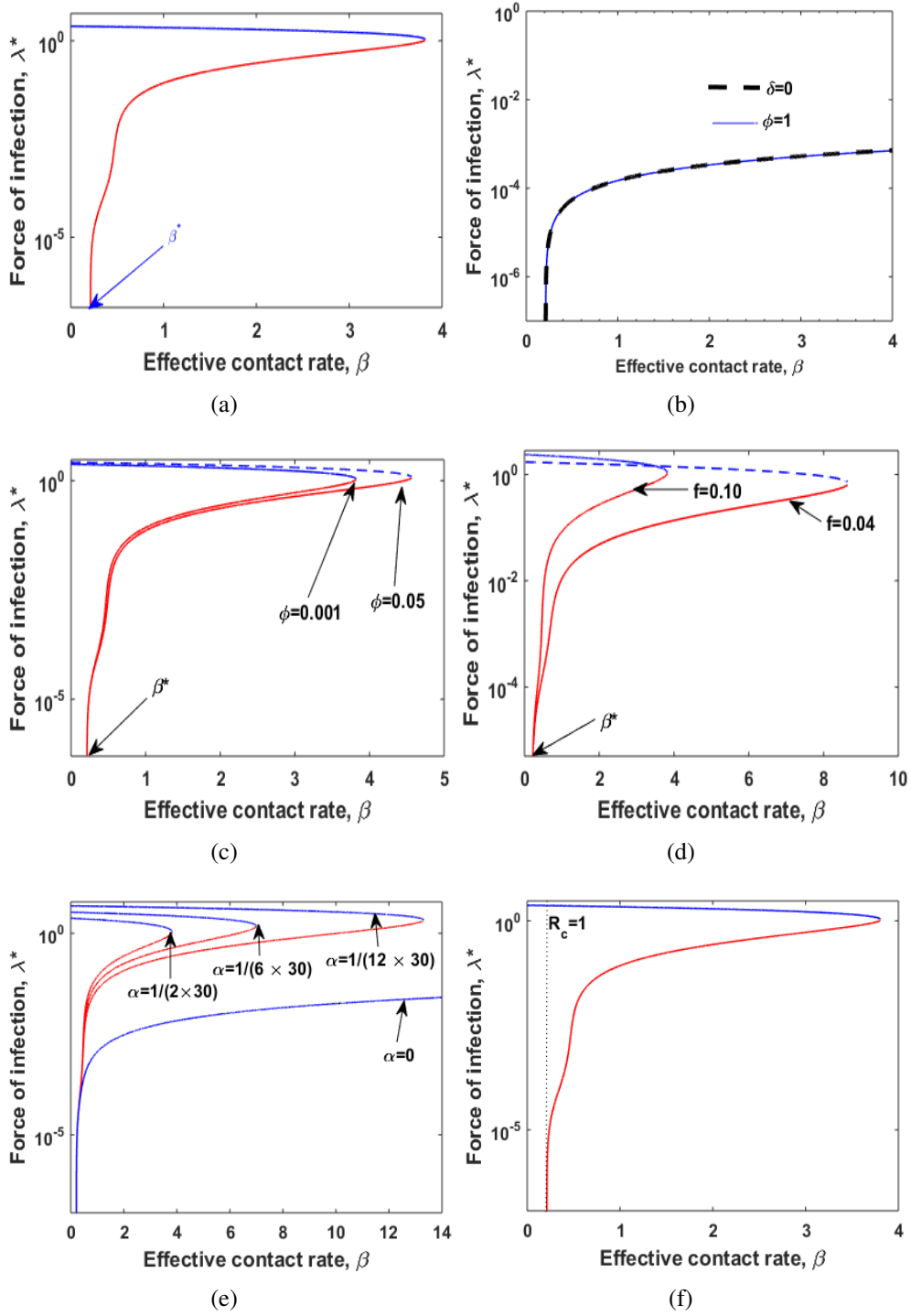


Figure 2: Illustrate type of bifurcation structures exhibited by the model system (2). Parameters used to generate figures are the baseline parameters depicted in Table 4 except those shown in the figures. In all the figures $\beta^* = 0.212$ correspond to $R_c = 1$. (a) Represents a reversed backward bifurcation phenomenon for $\delta = 0.5$ which correspond to $\delta(1 - \phi) = 0.4991 < \delta_c = 1.0004$. (b) Show the structural change of *reversed backward bifurcation* to the usual forward bifurcation whenever reinfection does not boost an individual infection-acquired immunity (i.e., $\phi = 1$) and when reinfection does not occur (i.e., $\delta = 0$). (c) Show the impact of increasing the proportion ϕ of recovered individuals with partial infection-acquired immunity at intermediate values ($0 < \phi < 1$). (d) Show effect of increasing parameter f ($0 < f < 1$). (e) Show the impact of varying the duration of infection-acquired immunity. (f) Illustrate a *reversed backward bifurcation* phenomenon can occur even when $\phi = 0$.

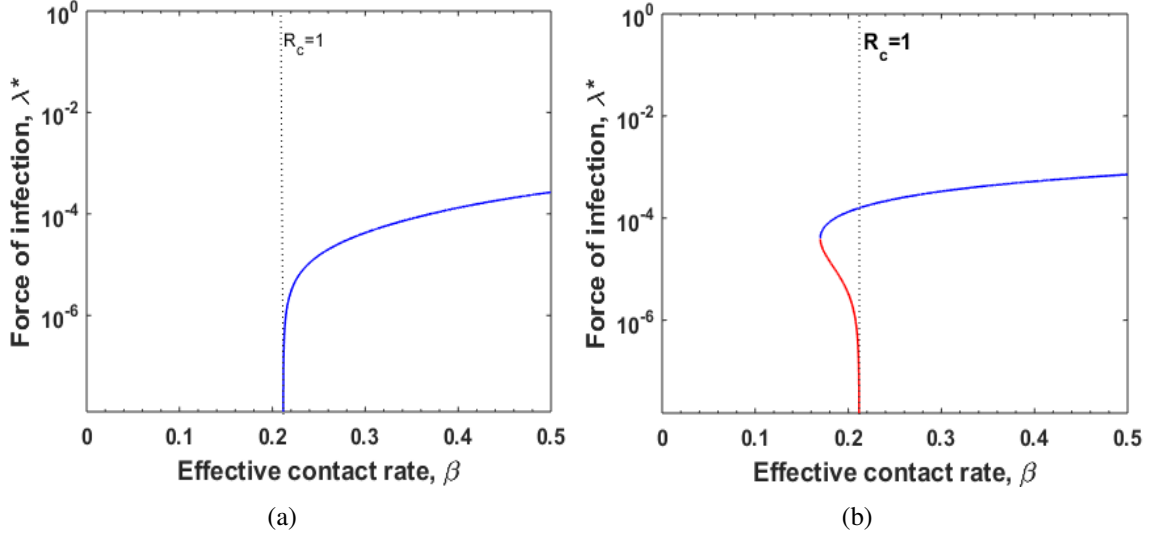


Figure 3: Illustrate the typical forward bifurcation and the backward bifurcation structures when the recovered individuals in R_2 class are assumed to acquire an everlasting infection-acquired immunity (i.e., $\alpha = 0$). The parameters used are the baseline parameters shown in Table 4. (a) Represents forward bifurcation when $\delta = 0.5$ which correspond to $\delta(1 - \phi) = 0.4991 < \delta_c = 1.0004$. (b) Represents backward bifurcation for $\delta = 2$ which corresponds to $\delta(1 - \phi) = 1.9980 > \delta_c = 1.0004$.

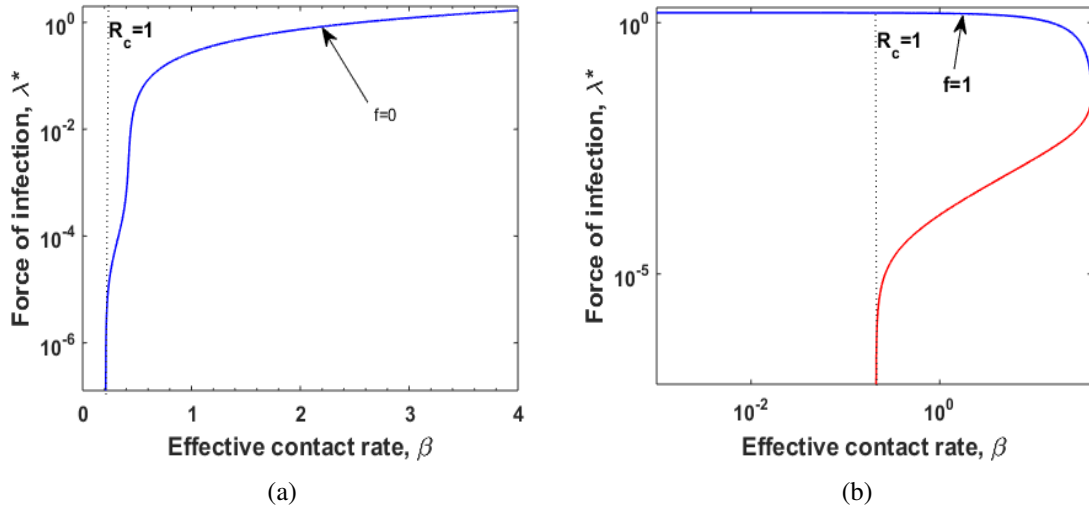


Figure 4: Illustration of the scenario where there is no heterogeneity in recovery among infected individuals. (a) Represents bifurcation structure for the case $f = 0$, i.e., infected individuals who do not succumb to COVID-19 all recover with partial/weak infection-acquired immunity and therefore progress to R_1 which consists of individuals who are prone to reinfection. Parameters used remain as the baseline parameters shown in Table 4 except $f = 0$ is shown in the figure. For a better view semi-logarithmic scale is used. (b) Represents bifurcation structure (pronounced *reversed backward bifurcation*) for the case $f = 1$, i.e., infected individuals who do not succumb due to COVID-19, all recover with strong temporary infection-acquired immunity. Parameters used remain as shown in the Table 4 except $f = 1$ is shown in the figure. For a better view a logarithmic scale is used on both axis.

5.9. Reinfection being more likely to occur than initial infection

Here we consider two scenarios; (a) a scenario where reinfection occur at the same rate as primary infection (initial infection) and (b) reinfection of recovered individuals with partial immunity occur at a higher rate in comparison to infection of susceptible individuals. Thus, fixing all the other parameters (baseline parameters) as shown in Table 4 while varying parameter δ we investigate these two cases. Figure 5(a) show that if reinfection occur at the same rate as infection of susceptible individuals then the phenomenon of a *reversed backward bifurcation* is preserved. However, if reinfection rate surpasses the rate of initial infection, then there is a structural change in the bifurcation structure as the *reversed backward bifurcation* switches to a *reversed hysteresis effect* as exhibited in Figures 5(b), 5(c) and 5(d) where δ values are $\delta = 2, \delta = 3, \delta = 4$, respectively. The appearance of a reversed hysteresis effect complicates COVID-19 transmission dynamics as there are multiple endemic equilibria (both stable and unstable) when $R_c < 1$ and when $R_c > 1$.

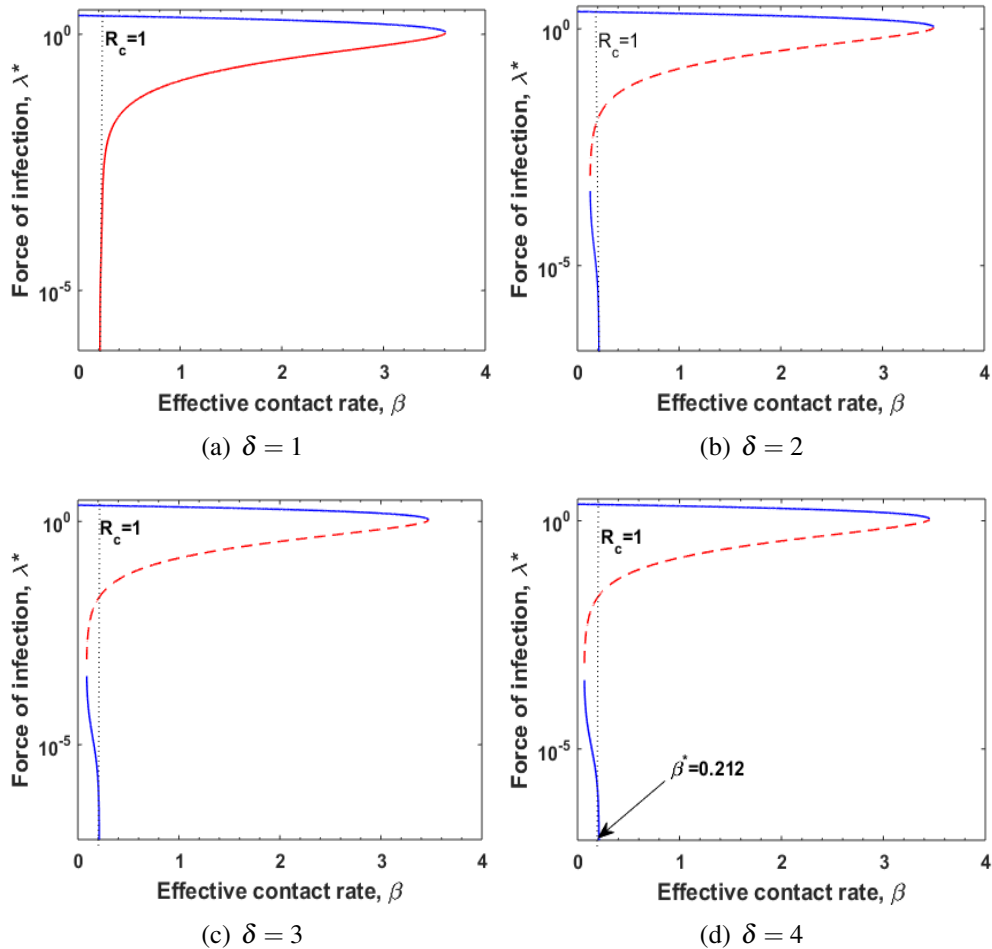


Figure 5: Depict the impact of readjusting the modification parameter that account for reinfection among recovered individuals with partial immunity such that $\delta \geq 1$. Parameter values used to generate the figures remain as baseline parameters shown in Table 4 except that β is varied within the interval $\beta \in [0.001, 4]$. Blue solid curves represent stable endemic curves while solid and dotted red curves represent unstable endemic curves. For a better view semi-logarithmic scales are used on all figures. (a) Represents the reversed backward bifurcation when $\delta = 1$. (b) Represents a reversed hysteresis effect which occur when $\delta = 2$ and $\delta(1 - \phi) = 1.9980 > \delta_c = 1.0004$. (c) Represents a reversed hysteresis effect when $\delta = 3$ and $\delta(1 - \phi) = 2.997 > \delta_c = 1.0004$. (d) Show a hysteresis effect bifurcation structure for $\delta = 4$ and $\delta(1 - \phi) = 3.9960 > \delta_c = 1.0004$.

5.10. Impact of non-pharmaceutical mitigation measures and proportion of boosted immunity on COVID-19 burden

Figure 6(a) depict that increasing parameters that account for non-pharmaceutical intervention (NPI) measures does lead to a decline in force of infection. Thus, if the general populace adhere to the NPI mitigation measures COVID-19 prevalence can be significantly reduced. Figure 6(a) show that if a larger proportion of recovered individuals with partial immunity transition to a class of recovered individuals with strong temporary immunity after reinfection, then COVID-19 prevalence declines (with λ^* being close to zero when parameter $\phi \rightarrow 1$).

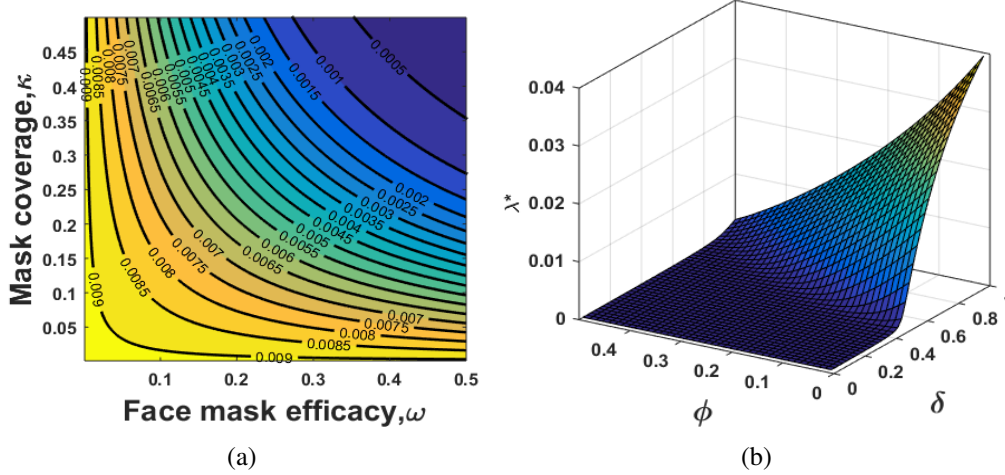


Figure 6: (a) Illustrate the contour plots of of face mask efficacy ω versus the face mask coverage κ for the force of infection (λ^*) at equilibrium. (b) Represents a 3-D figure showing the impact of varying proportion of boosted immunity and reinfection coefficient on the force of infection λ^* . Parameters used in both figures are the baseline parameters shown in Table 4.

6. Time series solutions

To understand the long-term dynamical behaviour of the formulated COVID-19 model system (2) we present several graphical representations to support our theoretical findings. Two broad scenarios will be considered; that is when the basic reproduction number is either less or greater than one. Except where mentioned, parameter values used for numerical simulations remain as shown in Table 4 (baseline parameter values) while the initial conditions used are $S(0) = 5000000, E(0) = 100, I(0) = 70, R_1(0) = 10, R_2(0) = 10$. Figure 7 (see Figures 7(a), 7(b), 7(c) and 7(d)) which presents the time evolution of COVID-19 model system (2) when the fundamental threshold is greater than unity depicts that COVID-19 will be endemic. Figure 7(d) show that COVID-19 will peak within a period of about 100 days and thereafter decline and settle at the equilibrium point.

It is important to note that the subpopulation of recovered individuals with weak immunity increases and stabilizes at equilibrium point (see Figure 7(c)) without decreasing. On one hand the subpopulation of recovered individuals with strong temporaly infection-acquired immunity increases then decreases before settling at the equilibrium point as depicted in Figure 7(d). The epidemiological implication of this decline among recovered individuals with

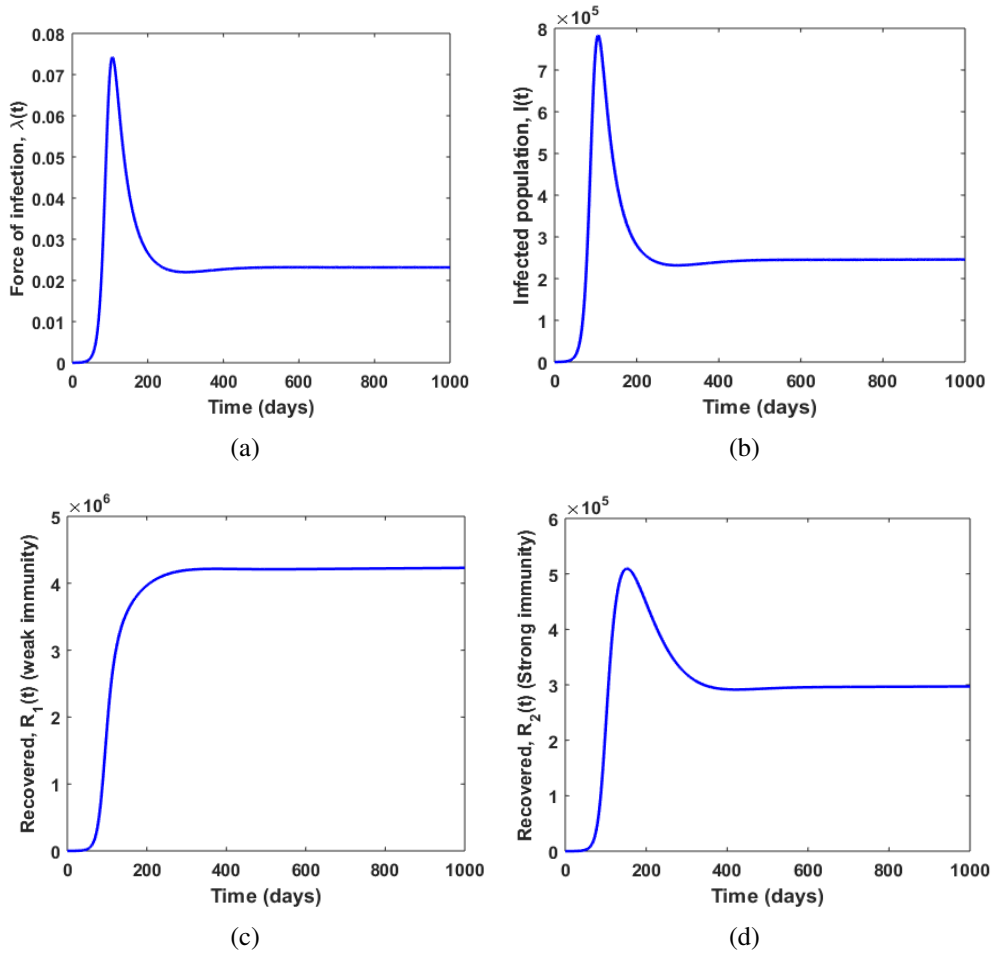


Figure 7: Illustration of COVID-19 transmission dynamics when the control reproduction number is greater than one. The parameter values used remain as shown in Table 4 except $\beta = 0.5$ which correspond to $R_c = 2.36 > 1$. Note that in all figures $\delta = 0.5$ and $\phi = 0.001$ which corresponds to $\delta(1 - \phi) = 0.4991 < \delta_c = 1.0004$.

strong immunity is because these individuals' infection-acquired immunity start to wane after some time (about six months). This is due to the fact that the infection-acquired immunity is not everlasting. Once they lose the infection-acquired immunity they transition to recovered individuals with weak/partial immunity. Consequently one would expect the R_1 class to increase, however there is no increase because individuals in R_1 class get reinfected and progress to either E class or revert to R_2 class.

Figure 8 show that whenever control reproduction number is below unity and the condition $\delta(1 - \phi) < \delta_c$, hold then COVID-19 will not become endemic as the trajectories approach zero as time elapses (see Figures 8(a) and 8(b)). Intriguingly when the parameters are chosen such that the condition $\delta(1 - \phi) < \delta_c$ is reversed (i.e., $\delta(1 - \phi) > \delta_c$) and the control reproduction number is below unity, the dynamical behaviour of the model system 2 yield a scenario where COVID-19 trajectories are determined by the size of the supplied initial conditions. This is the signature for the phenomenon of backward bifurcation as exhibited in Figure 3(b) where there is co-existence of both unstable and stable endemic equilibria when $R_c < 1$. In such scenario some supplied initial conditions are attracted to the stable endemic

equilibrium point while others are attracted to the basin of disease free equilibrium point. This is the case exhibited by Figures 9(a) and 9(b).

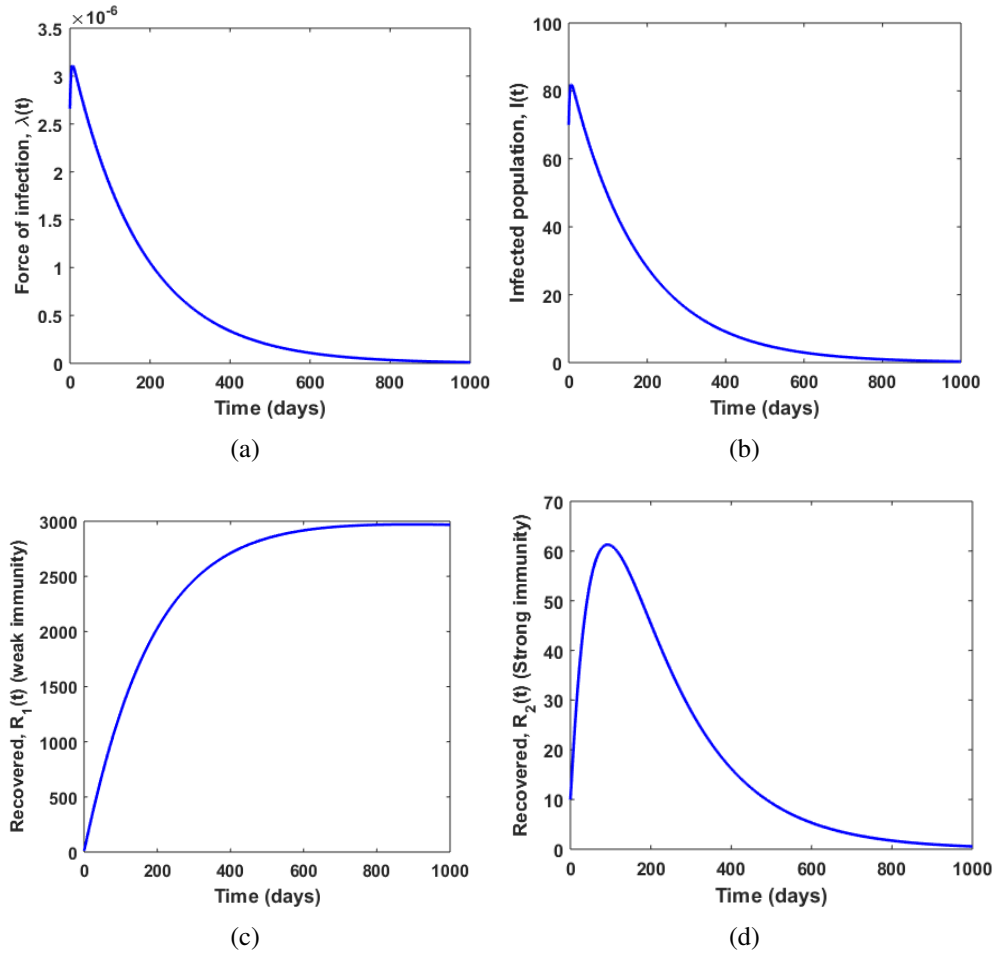


Figure 8: Illustration of COVID-19 transmission dynamics when the control reproduction number is less than one. Parameter values used remain as shown in Table 4 except $\beta = 0.2 (< \beta^* = 0.212)$ which corresponds to $R_c = 0.94 < 1$. All figures are generated when $\delta(1 - \phi) = 0.4991 < \delta_c = 1.0004$.

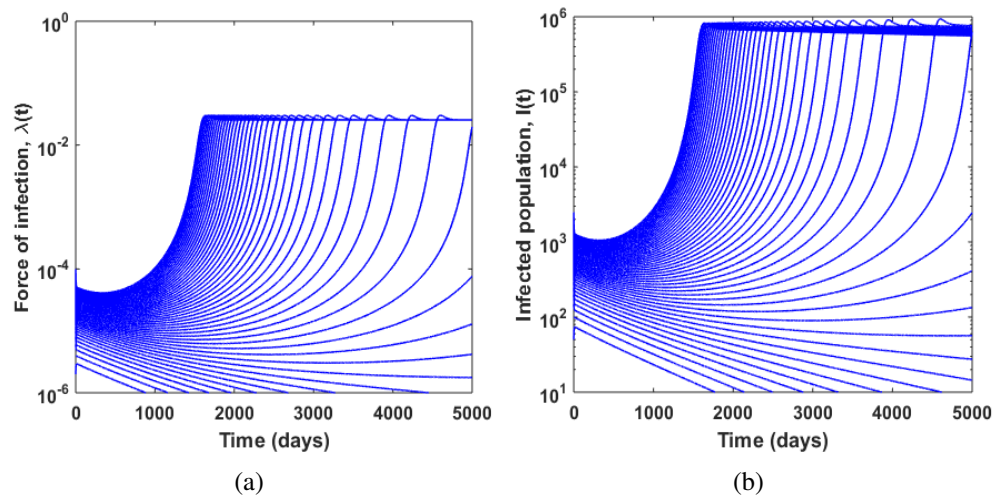


Figure 9: Illustration of the dependence of COVID-19 trajectories on the supplied initial conditions. The parameters used remain as indicated in Table 4, except $\beta = 0.209$ (which correspond to $R_c = 0.9874 < 1$), $\alpha = 1/(3 \times 30)$ and $\delta = 2$ (corresponding to $\delta(1 - \phi) = 1.9980 > \delta_c = 1.0004$). (a) Represent force of infection time series. (b) Represents infectious cases time series. For a better view a semi-logarithmic scale is used.

6.1. Effect of face mask efficacy versus face mask coverage

Figures 10(a) and 10(b), respectively show the impact of increasing face mask efficacy and face mask coverage on COVID-19 transmission dynamics. Face masks with high efficacy has a positive impact on curbing COVID-19. This is because there is a significant decline and delay of COVID-19 peak as face mask efficacy increases. In fact with just face mask efficacy of about 50% COVID-19 trajectory is attracted to the disease free equilibrium (see Figure 10(a) and also 3-D Figure 10(c)). The delay and decline of COVID-19 peak as a result of increasing mask efficacy suggest that medical practitioners should advice the general populace to use masks that have been demonstrated to render maximum protection against acquisition of COVID-19 as well as transmission of COVID-19. However, increasing face mask coverage does not significantly reduce or delay COVID-19 peak and also does not lead to eradication of COVID-19 (even when face mask coverage is about 100% - see Figure 10(b) and 3-D Figure 10(d)). The only positive impact of high mask coverage is the reduction of COVID-19 prevalence.

6.2. Impact of varying duration of infection-acquired immunity versus varying proportion of boosted immunity as a result of reinfection

Increasing duration of infection-acquired immunity does not reduce or delay COVID-19 peak as exhibited in Figure 10(e). However, longer duration of infection-acquired immunity does reduce COVID-19 prevalence and if infection-acquired immunity is permanent it may ultimately lead to COVID-19 dying out. This observation is crucial because if countries could have relied on natural immunity without incorporating pharmaceutical mitigation measures such as administration of vaccines, it could have been extremely difficult to contain COVID-19 proliferation. Figure 10(f) depict that if proportion of individuals whose infection-acquired immunity is boosted as result of reinfection (re-exposure to COVID-19) is increased, then there is a decline in the COVID-19 peak but it does not lead to flatening of the COVID-19 curve (i.e., delaying the COVID-19 peak). With over 50% of recovered individuals with partial immunity transitioning to R_2 class after reinfection, then COVID-19 endemic could have been eradicated within a period of approximately 200 days (see Figure 10(f)). However, this eradication could have been only possible if second episode of COVID-19 strengthens an individual previously infection-acquired immunity.

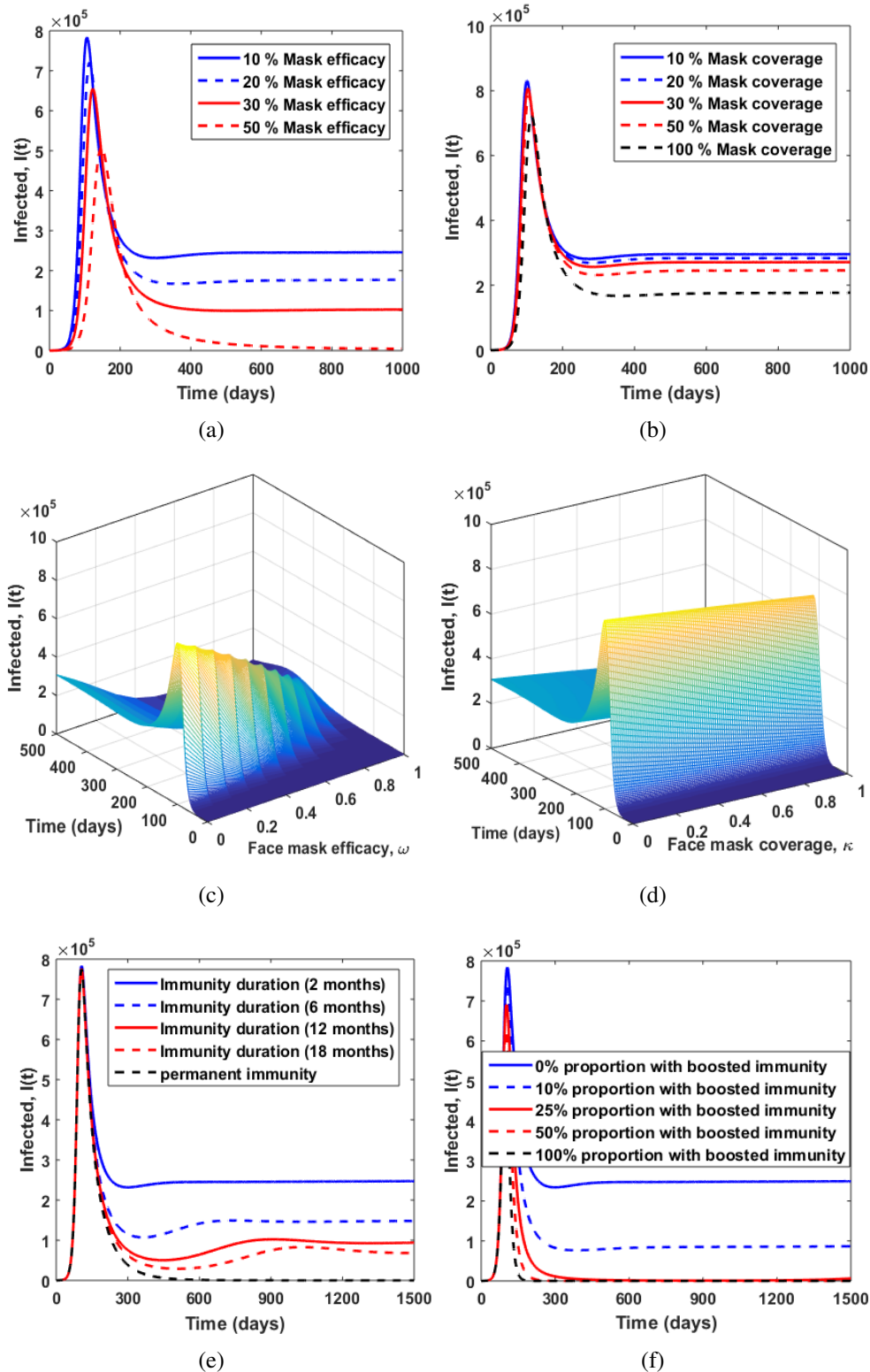


Figure 10: Illustrate time series solutions when different parameter values are varied. (a) Represent effect of high face mask efficacy. (b) Represents impact of increasing face mask coverage on COVID-19 transmission dynamics. (c) Represent a 3-D figure showing the effect of face mask efficacy on COVID-19 transmission dynamics when considering a larger interval of parameter ω values. (d) Represent a 3-D figure showing impact of mask coverage on a broader range of parameter κ values. (e) Represents impact of duration of infection-acquired immunity. (f) Represents impact of increasing proportion of recovered individuals whose immunity is boosted upon reinfection.

7. Discussion and conclusion

We designed an SEIR_{*i*} ($i \in \{1, 2\}$) mathematical model with the aim of investigating two key questions: (a) Whether immunological differences in infection-acquired immunity among recovered individuals can alter the dynamical behaviour of COVID-19 (b) If reexposure to COVID-19 boosts previously infection-acquired immunity (natural immunity), are there new epidemiological insights? The theoretical and numerical findings reveal that heterogeneity in infection-acquired immunity among both recovered cohorts (i.e., recovered individuals with partial immunity and recovered individuals with strong temporary immunity) can induce complex bistability phenomenon. That is the proposed COVID-19 model, shows that if there is a gradual loss of infection-acquired immunity among recovered individuals with strong immunity a *reversed backward bifurcation* phenomenon arises. This leads to a scenario where COVID-19 unfolds into two endemic curves when the control reproduction number is greater than one. These findings have not been documented in any existing COVID-19 literature.

Both analytical and numerical findings reveal that if the immunity acquired by recovered individuals with strong immunity is everlasting the *reversed backward bifurcation* is annihilated and the usual *forward bifurcation* emerges. However, under this scenario forward bifurcation occur only when primary infection is more likely than reinfection (i.e., $0 < \delta < 1$). Immediately the reinfection is more likely to occur ($\delta > 1$) than primary infection then, the *forward bifurcation* switches to the *backward bifurcation* phenomena. Under the assumption that upon reinfection with COVID-19, boosting of infection-acquired immunity among recovered individuals with partial immunity is perfect the *reversed backward bifurcation* structure transforms to *forward bifurcation*. Although, this is unlikely in a real life situation given there has been documented evidence of breakthrough infections after initial infection (or after vaccination), especially with new emerging COVID-19 variants Rahman et al. [4]. Further, *reversed backward bifurcation* is annihilated and *forward bifurcation* emerges if all infected individuals recover with partial infection-acquired immunity and *reversed backward bifurcation* is preserved if all infected individuals recover with strong infection-acquired immunity. These results may seem confounding but they are not surprising given recovered individuals with strong immunity have temporary infection-acquired immunity and over time their strong immunity wane. Subsequently reverting to recovered individuals with partial immunity who are prone to reinfection.

Moreover, a new type of bifurcation structure which we named *reversed hysteresis effect* emerges under the conditions that there is waning of infection-acquired immunity among individuals in R₂ class, boosted infection-acquired immunity is imperfect ($0 < \phi < 1$) and the likelihood of reinfection happening is higher than primary infection. The *reversed hysteresis effect* show existence of multiple endemic equilibria on either regions divided by the control reproduction number. Thus the presence of a *reversed hysteresis effect* might complicate intervention measures put in place to control COVID-19 proliferation given reducing control reproduction number below one will not be sufficient.

Further, we found that, longer duration of natural infection-acquired immunity does lead to the reduction of COVID-19 prevalence in the long-term (i.e., after about 200 days \approx 6 months). However, it does not lead to flattening of the COVID-19 epidemic curve. Thus, natural immunity alone cannot play a key role in alleviating COVID-19 crises especially

when countries have unlimited resources to cater for COVID-19 surge. However, non-pharmaceutical interventions (NPIs) measures such as wearing face masks with high effectiveness can lead to both flattening the COVID-19 curve as well as reducing COVID-19 prevalence. Our numerical results also stress that mask efficacy plays a significant role in COVID-19 reduction than mask coverage.

The findings in this paper suggests that boosted natural infection-acquired immunity as a result of reexposure can alter long-term COVID-19 transmission dynamics positively. However, as researchers across the globe continue to unravel the intricate transmission dynamics of COVID-19, perhaps there are questions worth noting. For instance, after grim projection and predictions of COVID-19 in some developing countries where there are inadequate health facilities, COVID-19 morbidity and mortality was far much below than the initial projections. And this raises an important question whether previous exposure to closely related subvariants of coronavirus could have played a key role in preventing spiralling of COVID-19 cases that could have resulted to overburdening of the available medical facilities.

Future direction of this paper could consider callibrating the proposed COVID-19 dataset to accurately determine the values of proportion that account for boosted immunity among recovered individuals with partial immunity as well as determinig the value of reinfection coefficient. Further, incorporating pharmaceutical mitigation measures such as vaccines can add insights regarding the interplay between naturally infection-acquired immunity and vaccine-induced immunity.

References

- [1] WHO Coronavirus (2019-nCoV) Report, Novel coronavirus (2019-ncov) situation report, World Health Organization (WHO), 2020. <https://source.coronaviruse/situation-reports/20200121-sitrep-1-2019-ncov.pdf>, . Accessed: 2020-01-20.
- [2] India's drugs experts approve Astrazeneca, local COVID vaccines. <https://www.reuters.com/article/health-coronavirus-india-vaccine/indias-drugs-experts-approve-astrazeneca-local-covid-vaccines-idUSKBN29707B>. Accessed: 2021-02-10.
- [3] WHO Coronavirus (COVID-19) Dashboard. <https://covid19.who.int/>, . Accessed: 2021-02-5.
- [4] S. Rahman, M. M. Rahman, M. Miah, M. N. Begum, M. Sarmin, M. Mahfuz, M. E. Hossain, M. Z. Rahman, M. J. Chisti, T. Ahmed, and S. E. Arifeen. Covid-19 reinfections among naturally infected and vaccinated individuals. *Scientific reports*, 12(1): 1–10, 2022.
- [5] R. M. Anderson and R. M. May. *Infectious diseases of humans: dynamics and control*. Oxford university press, 1992.
- [6] M. J. Keeling and P. Rohan. *Modelling infectious diseases in humans and animals*. Princeton University press, 2008.
- [7] A. Le, A. A. King, F. M. G. Magpantay, A. Mesbahi, and P. Rohani. The impact of infection-derived immunity on disease dynamics. *Journal of Mathematical Biology*, 83(6):1–23, 2021.

- [8] Katherine ME Turner, Elisabeth J Adams, Nigel Gay, Azra C Ghani, Catherine Mercer, and W John Edmunds. Developing a realistic sexual network model of chlamydia transmission in Britain. *Theoretical biology and medical modelling*, 3(1):1–11, 2006.
- [9] C. B. Hall, E. E. Walsh, C. E. Long, and K. C. Schnabel. Immunity to and frequency of reinfection with respiratory syncytial virus. *Journal of Infectious Diseases*, 163(4): 693–698, 1991.
- [10] K. N. A. Pangesti, M. Abd El Ghany, M. G. Walsh, A. M. Kesson, and G. A. Hill-Cawthorne. Molecular epidemiology of respiratory syncytial virus. *Reviews in medical virology*, 28(2):e1968, 2018.
- [11] E. O. Ohuma, E. A. Okiro, C. J. Ochola, R. Sande, P. A. Cane, G. F. Medley, C. Bottomley, and D. J. Nokes. The natural history of respiratory syncytial virus in a birth cohort: the influence of age and previous infection on reinfection and disease. *American journal of epidemiology*, 176(9):794–802, 2012.
- [12] Christian Holm Hansen, Daniela Michlmayr, Sophie Madeleine Gubbels, Kåre Mølbak, and Steen Ethelberg. Assessment of protection against reinfection with SARS-CoV-2 among 4 million PCR-tested individuals in Denmark in 2020: a population-level observational study. *The Lancet*, 397(10280):1204–1212, 2021.
- [13] J. M. Dan, J. Mateus, Y. Kato, K. M. Hastie, E. D. Yu, C. E. Faliti, A. Grifoni, S. I. Ramirez, S. Haupt, and A. Frazier. Immunological memory to SARS-CoV-2 assessed for up to 8 months after infection. *Science*, 371(6529), 2021.
- [14] A. M. Salman, I. Ahmed, M. H. Mohd, M. S. Jamiluddin, and M. A. Dheyab. Scenario analysis of COVID-19 transmission dynamics in Malaysia with the possibility of reinfection and limited medical resources scenarios. *Computers in biology and medicine*, 133:104372, 2021.
- [15] I. M. Wangari, S. Sewe, G. Kimathi, M. Wainaina, V. Kitemu, and W. Kaluki. Mathematical modelling of COVID-19 transmission in Kenya: a model with reinfection transmission mechanism. *Computational and Mathematical Methods in Medicine*, 2021, 2021.
- [16] S. A. Lauer, K. H. Grantz, Q. Bi, F. K. Jones, Q. Zheng, H. R. Meredith, A. S. Azman, N. G. Reich, and J. Lessler. The incubation period of coronavirus disease 2019 (COVID-19) from publicly reported confirmed cases: estimation and application. *Annals of internal medicine*, 172(9):577–582, 2020.
- [17] C. M. Batistela, D. P. F. Correa, A. M. Bueno, and J. R. C. Piqueira. SIRSi compartmental model for COVID-19 pandemic with immunity loss. *Chaos, Solitons & Fractals*, 142:110388, 2021.
- [18] A. K. Saha, C. N. Podder, and A. M. Niger. Dynamics of novel COVID-19 in the presence of co-morbidity. *Infectious Disease Modelling*, 7(2):138–160, 2022.
- [19] H. J. Wearing and P. Rohani. Estimating the duration of pertussis immunity using epidemiological signatures. *PLoS pathogens*, 5(10):e1000647, 2009.
- [20] W. O. Kermack and A. G. McKendrick. A contribution to the mathematical theory of epidemics. *Proceedings of the royal society of London. Series A, Containing papers of a mathematical and physical character*, 115(772):700–721, 1927.
- [21] W. O. Kermack and A. G. McKendrick. Contributions to the mathematical theory of epidemics. ii.-the problem of endemicity. *Proceedings of the Royal Society of London. Series A, containing papers of a mathematical and physical character*, 138(834):55–83, 1932.
- [22] V. Lakshmikantham, S. Leela, and A. A. Martynuk. *Stability analysis of nonlinear systems*. Springer, 1989.

- [23] H. W. Hethcote. The mathematics of infectious diseases. *SIAM review*, 42(4):599–653, 2000.
- [24] O. Diekmann, J. A. P. Heesterbeek, and J. A. J. Metz. On the definition and the computation of the basic reproduction ratio r_0 in models for infectious diseases in heterogeneous populations. *Journal of mathematical biology*, 28(4):365–382, 1990.
- [25] P. Van den Driessche and J. Watmough. Reproduction numbers and sub-threshold endemic equilibria for compartmental models of disease transmission. *Mathematical biosciences*, 180(1-2):29–48, 2002.
- [26] C. Castillo-Chavez and B. Song. Dynamical models of tuberculosis and their applications. *Math. Biosci. Eng*, 1(2):361–404, 2004.
- [27] C. N. Ngonghala, E. Iboi, S. Eikenberry, M. Scotch, C. R. MacIntyre, M. H. Bonds, and A. B. Gumel. Mathematical assessment of the impact of non-pharmaceutical interventions on curtailing the 2019 novel coronavirus. *Mathematical biosciences*, 325:108364, 2020.
- [28] S. Y. Tchoumi, H. Rwezaura, and J. M. Tchuenche. Dynamic of a two-strain covid-19 model with vaccination. *Results in Physics*, 39:105777, 2022.
- [29] S. M. Garba, J. M. Lubuma, and B. Tsanou. Modeling the transmission dynamics of the covid-19 pandemic in south africa. *Mathematical biosciences*, 328:108441, 2020.
- [30] S. Mwalili, M. Kimathi, V. Ojiambo, D. Gathungu, and R. Mbogo. Seir model for covid-19 dynamics incorporating the environment and social distancing. *BMC Research Notes*, 13(1):1–5, 2020.
- [31] L. Lin, Y. Zhao, B. Chen, and D. He. Multiple covid-19 waves and vaccination effectiveness in the united states. *International journal of environmental research and public health*, 19(4):2282, 2022.